

Study on wind load characteristics and aeroelastic performance of high-rise buildings based on the measured urban wind field

Z. Han¹, B. Li^{1,2}, C. Li¹, X. X. Zhang¹

¹ School of Civil Engineering, Beijing Jiaotong University, Beijing, China,
19115019@bjtu.edu.cn (Z.H); 16115322@bjtu.edu.cn (C.L); 18121167@bjtu.edu.cn (X.X.Z)

² Beijing's Key Laboratory of Structural Wind Engineering and Urban Wind Environment,
Beijing, China, boli@bjtu.edu.cn (B.L)

SUMMARY:

To investigate wind load characteristics and aeroelastic performance of high-rise buildings in the urban central wind field. The measured wind speed data observed continuously from the Beijing Meteorological Tower during 2013-2017 was selected, and the power-law was used to fit the measured wind profile based on the layered structure of the urban boundary layer. Wind-induced effects of high-rise buildings with 15 kinds of shapes in B, D (suburban terrain and urban terrain in the load code) and measured wind fields were studied by carrying out the rigid model pressure test and the aeroelastic model test in a wind tunnel. The researches show that the power exponent of the measured wind field is 0.35. The mean wind velocity profile is similar to the D wind field, while the turbulence profile is larger than that of the D wind field. Meanwhile, the fluctuating wind load of the large side ratio building is significantly enhanced in the measured wind field. The building with each shape configuration has good aeroelastic performance in the measured field, and the across-wind wind-induced response is mainly dominated by random buffeting indicating the advantages and disadvantages of the building shape can be judged by the corresponding aerodynamic performance.

Keywords: measured wind field, aerodynamic force, across-wind wind-induced response

1. INSTRUCTIONS

The wind profile is a main parameter affecting the wind-induced effect of high-rise buildings, and high-rise buildings with different shapes have different sensitivity to the wind profile. Davenport (1960) gave an empirical power-law wind profile model, which has been widely used because of its simplicity and practicality. Many scholars have studied the impact of the power-law wind profile on the wind-induced effect of high-rise buildings with varying shapes (Choi and Kanda, 1993; Kim and Kanda, 2010, 2013; Quan et al., 2016; Hu et al., 2017). However, most high-rise buildings are located in the urban centre, which has a complex underlying surface structure making the vertical direction of the urban boundary layer form a special layered structure (Li et al., 2021; Zhang et al., 2022). Its characteristics are different from the boundary layer naturally formed on the uniform rough surface. At present, the wind field selection of high-rise buildings in wind resistance design depends on the empirical wind field model in the code. Few works of literature have further investigated the wind-induced effect of high-rise buildings in the measured urban wind field.

To make up for this deficiency, the measured wind speed data observed continuously from the Beijing Meteorological Tower during 2013-2017 was selected in this paper. Based on the layered structure of the urban boundary layer, the power-law was used to fit the measured wind profile. Moreover, the measured wind field, as well as B (suburban terrain) and D (urban terrain) wind fields in the load code were simulated in the wind tunnel. Then, wind-induced effects of high-rise buildings with 15 kinds of shapes under three wind fields were studied by carrying out the rigid model pressure test and the aeroelastic model test in the wind tunnel, which provided references for wind resistance design of practical projects.

2. THE MEASURED WIND FIELD

The 325-meter-tall Beijing Meteorological Tower (BMT) is located in north-central Beijing (39°58'N, 116°22'E). The BMT has a total of 15 observation platforms, among which three-dimensional ultrasonic anemometers with a sampling frequency of 10 Hz are arranged at the heights of $z=8$ m, 16 m, 32 m, 47 m, 64 m, 80 m, 140 m, 200 m and 280 m (Fig.1(a)). The measured wind speed data was obtained from these nine heights during 2013-2017 and was divided with a time interval of 10-min. The power-law was used to fit the measured wind profile, and the result was compared with B and D wind fields in the load code. (Fig.1(b) and 1(c))

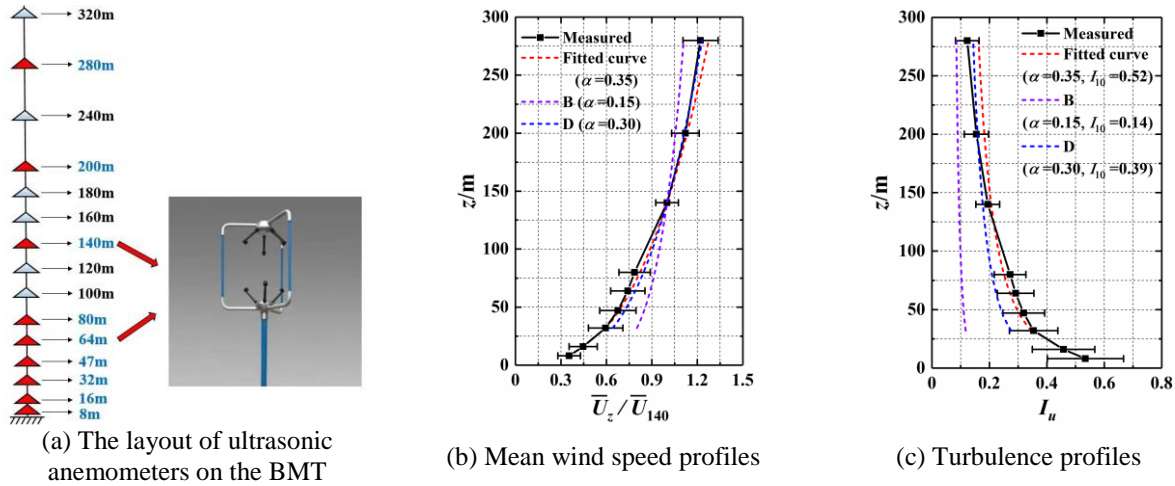


Figure 1. Comparison of the measured wind field with B and D wind fields in the load code

3. WIND TUNNEL TEST

Three wind fields introduced in the section 2 were simulated in the BJ-1 wind tunnel at Beijing Jiaotong University. The test models were 15 kinds of high-rise buildings including a square column, all of which were 400 mm high, with a scale ratio of 1:1000. Among them, the rigid models (Fig.2(a)) were three buildings with side ratios $L/D=1$, 2 and 4, respectively while the aeroelastic models (Fig.2(b)) were 13 kinds of buildings with different shape configurations. The aeroelastic model was pivoted at its base with a gimbal arrangement and was restrained by horizontal springs. The mass of the model was adjusted to ensure that the moment of inertia of all models was similar. Meanwhile, the across-wind natural frequencies of each model were also similar under the same springs. The structural damping was simulated via oil damping, and the across-wind adjustment range was about 0.4%~1% in this paper.

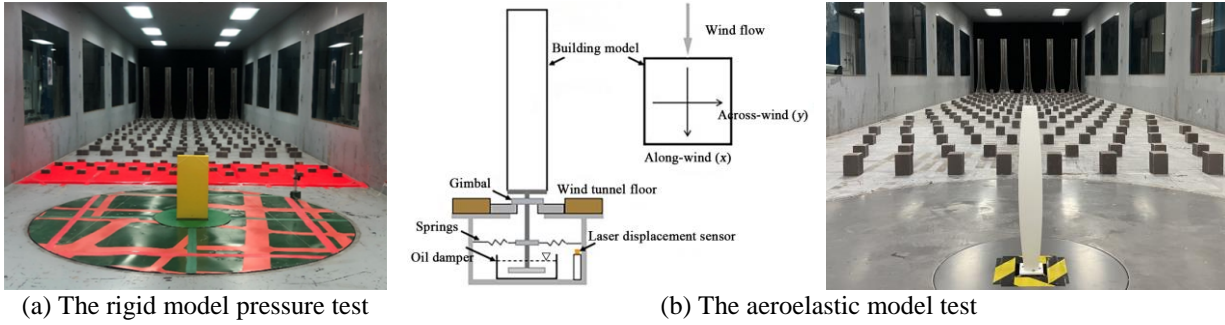


Figure 2. Experiment setup and models

4. RESULTS AND DISCUSSIONS

4.1. Local Wind Force Coefficient

The mean (\bar{C}_x) and fluctuating (C'_x, C'_y, C'_t) local wind force coefficients along the height of buildings under 90° wind direction are shown in Fig.3. It is depicted that for the building with $L/D=1$, the local wind force coefficient in the measured wind field is similar to the D wind field, while for the building with $L/D=4$, the fluctuating local wind force coefficient in the measured wind field is significantly larger than that of the D wind field.

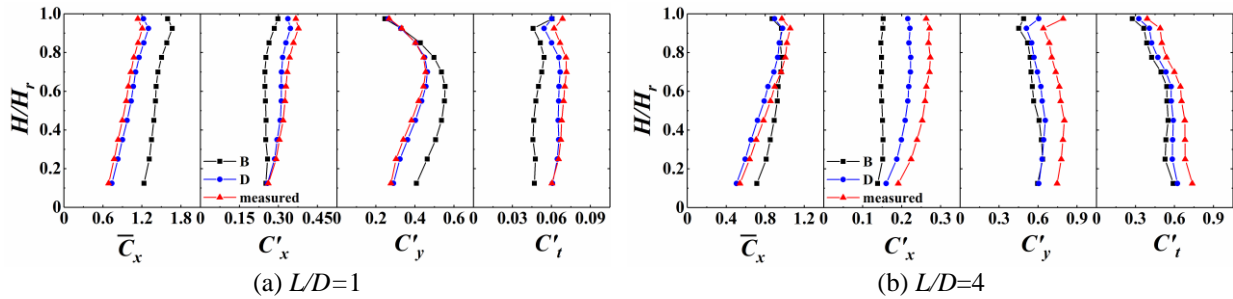
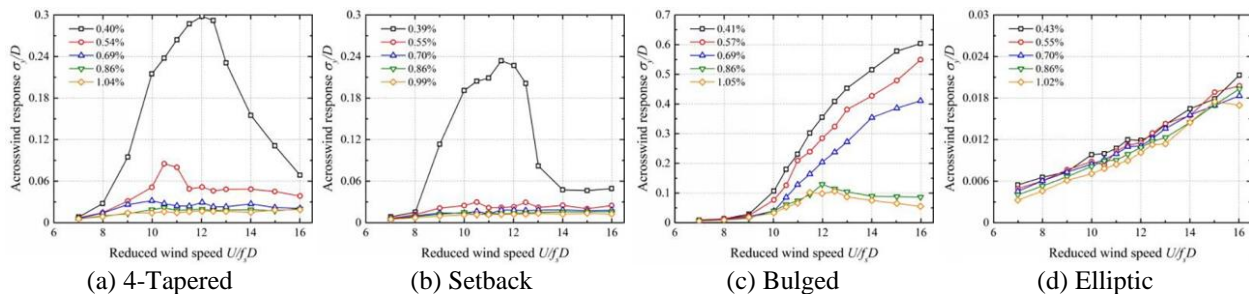


Figure 3. Distribution of local wind force coefficients along the height of buildings in different wind fields

4.2. Across-wind Displacement Response

Fig.4 shows the standard deviation of the across-wind displacement response of some high-rise buildings with different damping ratios in the B and measured wind fields. It is noticeable that under the measured wind field, the increase of the incoming turbulence inhibits the across-wind vortex-induced vibration of the structure. As a result, the across-wind fluctuating response is significantly smaller than that of in the B wind field and is mainly dominated by random buffeting.



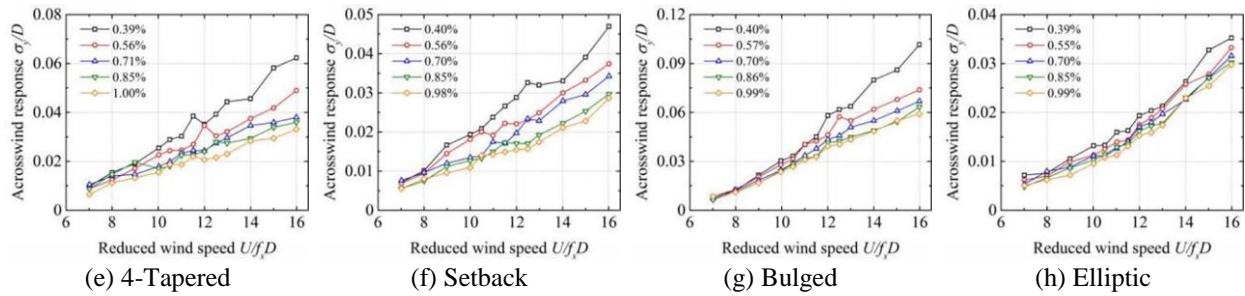


Figure 4. The standard deviation of the across-wind displacement response of some high-rise buildings with different damping ratios in the B (a-d) and measured (e-f) wind fields.

5. CONCLUSIONS

1. The power exponent of the measured wind field fitted by the power-law is 0.35. The mean wind velocity profile is similar to the D wind field, while the turbulence profile is larger than that of the D wind field.
2. Compared with the wind load in B and D wind fields, the measured wind field has less effect on the mean wind load of buildings but a greater effect on the fluctuating wind load. Moreover, with the increase of the building side ratio, the fluctuating wind load is significantly enhanced in the measured wind field.
3. The building with each shape configuration has good aeroelastic performance in the measured wind field, and the across-wind response is mainly dominated by random buffeting which is related to the flow turbulence. Therefore, the advantages and disadvantages of the building shape can be judged by the corresponding aerodynamic performance in the measured wind field.

ACKNOWLEDGEMENTS

This work is funded by the National Natural Science Foundation of China (51878041) and the 111 project of the Ministry of Education and the Bureau of Foreign Experts of China (B13002).

REFERENCES

- Choi, H. and Kanda, J., 1993. Proposed formulae for the power spectral densities of fluctuating lift and torque on rectangular 3-D cylinders. *Journal of Wind Engineering and Industrial Aerodynamics* 46/47, 507-516.
- Davenport, A. G., 1960. Rationale for determining design wind velocities. *Journal of the Structural Division, American Society of Civil Engineers* 86, 39-68.
- Hu, G., Hassanli, S., Kwok, K. C. S., and Tse, K. T., 2017. Wind-induced responses of a tall building with a double-skin façade system. *Journal of Wind Engineering and Industrial Aerodynamics* 168, 91-100.
- Kim, Y. C. and Kanda, J., 2010. Characteristics of aerodynamic forces and pressures on square plan buildings with height variations. *Journal of Wind Engineering and Industrial Aerodynamics* 98, 449-465.
- Kim, Y. C. and Kanda, J., 2013. Wind pressures on tapered and set-back tall buildings. *Journal of Fluids and Structures* 39, 306-321.
- Li, B., Li, C., Yang, Q. S., Tian, Y. J., and Zhang, X. X., 2021. Full-scale wind speed spectra of 5-year time series in urban boundary layer observed on a 325m meteorological tower. *Journal of Wind Engineering and Industrial Aerodynamics* 218, 104791.
- Quan, Y., Cao, H. L., and Gu, M., 2016. Effects of turbulence intensity and exterior geometry on across-wind aerodynamic damping of rectangular super-tall buildings. *Wind and Structures* 22, 185-209.
- Zhang, X. X., Li, B., Zhang, S., Yang, Q. S., and Tian, Y. J., 2022. Characteristics of wind field in urban boundary layer based on measured data in central Beijing. *Journal of Building Structures* 43, 109-117. (in Chinese)